Xiaobo Qu, Yingkun Hou, Fan Lam, Di Guo, Zhong Chen. Magnetic resonance image reconstruction using similarities learnt from multi-modal images, 2013 IEEE China Summit and International Conference on Signal and Information Processing-ChinaSIP'13, 6th – 10th , July, 2013, pp.264-268.

MAGNETIC RESONANCE IMAGE RECONSTRUCTION USING SIMILARITIES LEARNT FROM MULTI-MODAL IMAGES

Xiaobo Qu[1], Yingkun Hou[2], Fan Lam[3], Di Guo[4], Zhong Chen[1]

[1]Department of Electronic Science, Xiamen University, Xiamen 361005, China
[2]School of Information Science and Technology, Taishan University, Taian 271021, China
[3]Department of Electrical and Computer Engineering, University of Illinois at Urbana-Champaign, Urbana, IL 61801, USA
[4]School of Computer and Information Engineering, Xiamen University of Technology, Xiamen 361024, China

ABSTRACT

Compressed sensing has shown great potential to speed up magnetic resonance imaging (MRI) assuming the image is sparse and compressible in a transform domain. Conventional methods typically use a pre-defined sparsifying transform such as wavelets or finite difference, which sometimes does not lead to a sufficient sparse representation. In this paper, we design a patch-based nonlocal operator (PANO) to model the sparsity between image patches. The linearity of PANO allows us to establish a general formulation to reconstruct magnetic resonance image from undersampled data and provides feasibility to incorporate prior information learnt from guide images. To demonstrate the feasibility and performance of PANO, learning similarities from multi-modal images are presented to significantly improve the reconstructed images over conventional redundant wavelets in terms of visual quality and reconstruction errors.

Index Terms— MRI, Fast imaging, compressed sensing, nonlocal operator, multi-modality

1. INTRODUCTION

Magnetic resonance imaging (MRI) is widely used in the clinical diagnosis but limited by its data acquisition speed. Compressed sensing MRI (CS-MRI) has shown promising results to speed up the imaging assuming magnetic resonance (MR) images are sparse/highly compressible in a certain transform domain [1]. Typical transforms used in CS-MRI are wavelets, which is optimal for piece-smooth features, and finite difference, which is optimal for piece-wise constant features. Allowing the transform to sparsely represent other image features, contourlets [2] and high order total variation [3] are previously introduced in to MR image reconstruction. These transforms could be combined to further improve the reconstruction [1, 4].

A sparsifying transform or dictionaries learnt from undersampled data or prior images have shown great potential to reduce the reconstruction error. For example, dictionaries could be learnt from fully sampled image [5] or undersampled data [6]. If a guide image, indicating some image features of target image to be reconstructed, is available, the pixel sorting information [7, 8], geometric information [9] or the relationship between guide and target images can also be modeled [10] to improve the reconstruction.

Recently, the nonlocal processing has been introduced for MRI reconstruction to make use of the similarity of image patches [11-14]. Differences between neighboring patches are penalized. The sparsity originated from the similarity of image patches was exploited to reconstruct images from undersampled Fourier measurements in [15, 16]. It has been shown that edges are better preserved for these methods. However, MR image are reconstructed following an algorithm without a rigorous reconstruction model, which makes it hard to trade the data consistency and sparsity, as well as incorporate other prior information.

In this paper, we first establish a general patch-based nonlocal operator (PANO) to model the sparsity between image patches. The linearity of PANO allows us to establish a general reconstruction formulation and tradeoff between the sparsity of patches and the data consistency. Using PANO in formulation also provides the flexibility to incorporate other knowledge, e.g. prior information from a guide image, into the reconstruction. To demonstrate the feasibility of PANO, learning similarities from multi-modal images are presented to significantly improve the reconstructed images in terms of visual quality and reconstruction errors.

2. PATCH-BASED NONLOCAL OPERATOR

In this section, the linear operator PANO will be defined and undersampled MR image reconstruction will be presented.

2.1 Definition of PANO

Patch grouping is shown in Fig. 1. For a given image $\mathbf{x} \in \mathbb{C}^N$, we first decompose it into patches with fixed size $L \times L$. Let $\mathbf{P}_i$ defines the patch decomposition, and the i^{th} patch $\mathbf{b}_i \in \mathbb{C}^{L^2}$ is expressed as $\mathbf{b}_i = \mathbf{P}_i \mathbf{x}$. The v_j group of image patches is denoted as $\mathbf{R}_{v_j} \mathbf{b}_i$ where $v_j = \{i_1, \cdots, i_Q\}$ stores the index of patches. Let $\mathbf{\Psi}_{3D}$ be a 3D transform, we define the nonlocal operator PANO as

$$\mathbf{A}_j = \mathbf{\Psi}_{3D} \mathbf{R}_{v_j} \mathbf{P}_i . \tag{1}$$

If only one patch is available in a group, $\mathbf{\Psi}_{3D}$ is reduced to a 2D sparsifying transform, e.g. discrete cosine transform or Haar wavelet transform.

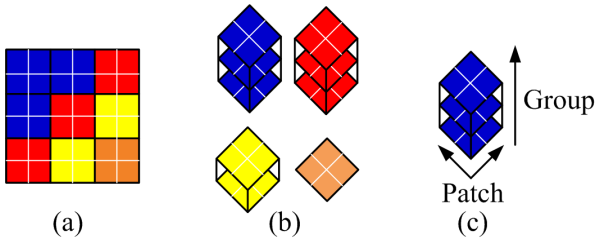

Fig.1. Group image patches. (a) An image with 6×6 pixels, (b) four groups of patches, (c) the patch and group dimension.

An optimal grouping is expected to produce sparse coefficients

$$\boldsymbol{\alpha}_j = \mathbf{A}_j \mathbf{x} . \tag{2}$$

The adjoint operator $\mathbf{A}_j^T$ is $\mathbf{A}_j^T = \mathbf{P}_i^T \mathbf{R}_{v_j}^T \mathbf{\Psi}_{3D}^T$ and it satisfies

$$\sum_j^J \mathbf{A}_j^T \mathbf{A}_j = c\mathbf{O} = c \begin{bmatrix} o_1 & 0 & \cdots & 0 & 0 \\ 0 & \ddots & \vdots & \iddots & 0 \\ \vdots & \cdots & o_n & \cdots & \vdots \\ 0 & \iddots & \vdots & \ddots & 0 \\ 0 & 0 & \cdots & 0 & o_N \end{bmatrix}, \tag{3}$$

if $\mathbf{\Psi}_{3D}$ is an orthogonal transform. o_n is a counter indicating the times of the n^{th} pixel are grouped and c is the overlap factor if overlapping patches are used [9]. Therefore, an image is estimated from PANO coefficients according to

$$\hat{\mathbf{x}} = \frac{1}{c} \mathbf{O}^{-1} \sum_{j=1}^J \mathbf{A}_j^T \boldsymbol{\alpha}_j . \tag{4}$$

Given the definition of PANO, we are now able to establish a general reconstruction formulation.

2.2 Reconstruction model using PANO

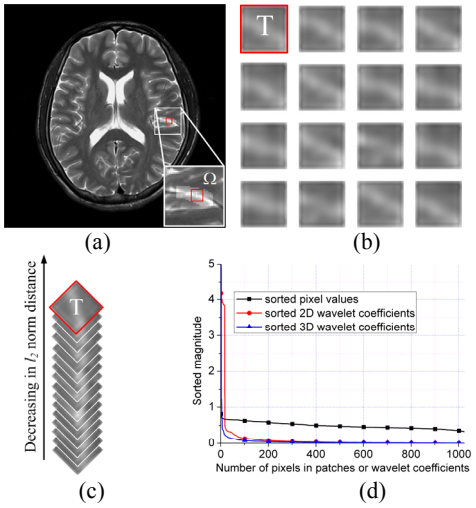

Fig.2. Illustration of the similar patches found via block matching and the sparsity results in. (a) A search region Ω with $D \times D = 39 \times 39$ and the reference patch $\mathbf{T}$ with $L \times L = 8 \times 8$, (b) $Q = 16$ similar patches found by the ℓ_2 norm distance measure with patch size $L = 8$, (c) 3D array stacked from the similar patches, and (d) curves for decay of pixel values, 2D and 3D wavelet coefficients.

Assuming that $\boldsymbol{\alpha}_j$ is sparse, we propose to reconstruct the MR image from undersampled k-space data by solving the following problem

$$\hat{\mathbf{x}} = \arg\min_{\mathbf{x}} \sum_{j=1}^J \left\| \mathbf{A}_j \mathbf{x} \right\|_1 + \frac{\lambda}{2} \left\| \mathbf{y} - \mathbf{F}_{\mathbf{U}} \mathbf{x} \right\|_2^2 \tag{5}$$

where the term $\sum_{j=1}^J \left\| \mathbf{A}_j \mathbf{x} \right\|_1$ promotes the sparsity and the term $\left\| \mathbf{y} - \mathbf{F}_{\mathbf{U}} \mathbf{x} \right\|_2^2$ enforces the data consistency. λ trades the sparsity with the data consistency. $\mathbf{F}_{\mathbf{U}} = \mathbf{U}\mathbf{F}$ means that a undersampling operator $\mathbf{U} \in \mathbb{R}^{M \times N}$ multiplies on a unitary Fourier transform $\mathbf{F} \in \mathbb{R}^{N \times N}$ [1-9].

To solve the problem in Eq. (5), we use the variable splitting and quadratic penalty technique proposed in [17] because of its advantage in handling the ℓ_1 norm-based optimization with image patches [5, 9]. Details are omitted here due to the limited space.

2.3 Choice of grouping

In this paper, similar patches are grouped to produce sparse coefficients since it shows great potentials to improve the MR image reconstruction [15, 16].

Fig. 2(a) illustrates how to group similar patches. For a search region Ω and the reference patch $\mathbf{T}$, we measure the similarity between the reference patch and a candidate patch using the ℓ_2 norm distance. $Q-1$ candidates with the

smallest distance are selected as similar patches. This process is called block matching [18]. Since the available search region can be as large as the entire image, the similar patches are not limited to a local region. Thus, the similarity is nonlocal.

Performing the 3D Haar wavelet transform on this group, spares coefficients are produced due to the similarity of these patches. An example is shown in Fig. 2. 15 similar patches and the reference patch are grouped in Fig. 2(c). Fig. 2(d) shows that 3D Haar wavelet coefficients of the 3D array decay much faster than the coefficients of 2D Haar wavelet and the pixel values of these patches. This observation implies that 3D Haar wavelets can provide sparser vectors of these grouped patches than 2D Haar wavelets.

3. RESULTS

To demonstrate the feasibility of PANO, two examples, which learn similarities from an intermediate image or another modal image, will be presented in this section. The flowchart of the reconstruction is shown in Fig.3.

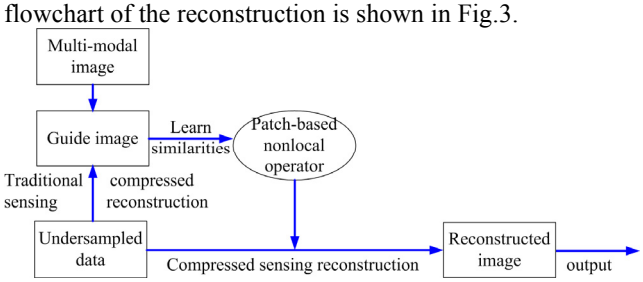

Fig.3. Flowchart of PANO-based undersampled magnetic resonance image reconstruction.

The multi-modal MR images shown in Fig. 4 are T1 and T2 weighted MR images [19]. These images are with 1mm^3 voxel resolution and 8 bit quantization from the Brainweb phantom [20]. Undersampling is simulated by acquiring partial phase encodings as shown in Fig. 4(b). The realistic multi-modal MR images shown in Fig. 5 are T1 and T2 weighted MR images, which are acquired from a healthy volunteer at a 1.5T Philips MRI scanner with sequence parameters (T1-weighted image: TR/TE=1700/390ms; T2-weighted image: TR/TE=3000/800ms, both images are with 230×230 mm field of view, 5 mm slice thickness). Undersampling is simulated by acquiring partial phase encodings as shown in Fig. 5(b).

To evaluate the reconstruction error, we use the relative ℓ_2 norm error (RLNE) [9] defined as

$$e(\hat{\mathbf{x}}) = \left\|\hat{\mathbf{x}} - \tilde{\mathbf{x}}\right\|_2 / \left\|\tilde{\mathbf{x}}\right\|_2 \qquad (6)$$

to measure the difference of reconstructed image $\hat{\mathbf{x}}$ and fully sampled image $\tilde{\mathbf{x}}$.

Parameters of PANO are $D \times D$=39×39, $L \times L$=8×8, and Q=8. The regularization parameter is λ=10^6 for PANO and shift-invariant wavelets (SIDWT) used as sparsifying transform in conventional CS-MRI method. SIDWT is chosen since it outperforms the original CS-MRI [1] and is with fast computation.

The programs run on dual core 2.2 GHz CPU laptop with 3 GB RAM. The proposed method requires 4 minutes to reconstruct one image for a given similarity.

3.1 Learn similarities from an intermediate image

The guide image is pre-reconstructed using shift-invariant Haar wavelets [9]. Comparing Fig. 4(c) with Fig. 4(d), PANO significantly remove the artifacts and reduce the reconstruction error by learning similarities from the images. However, some are still presented in the tagged place of Fig. 4(d) when PANO is used.

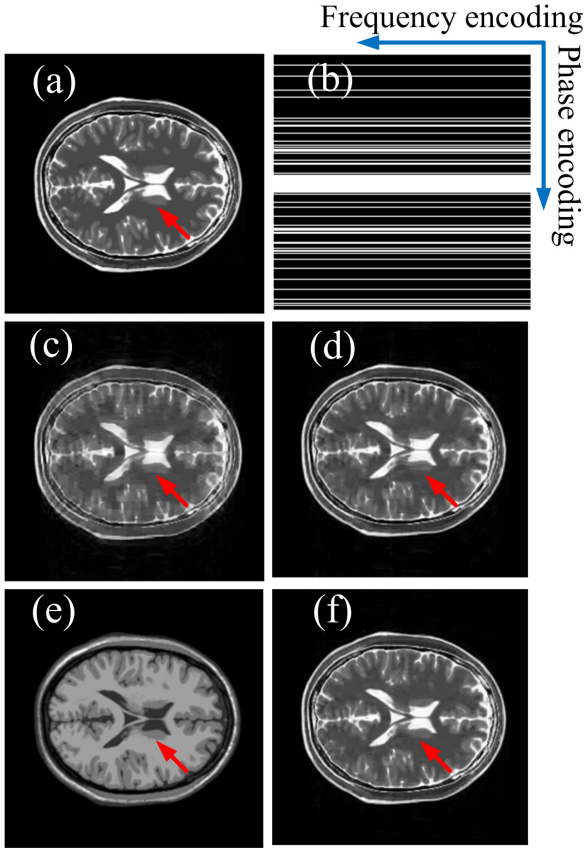

Fig.4. Reconstructed images on simulated data. (a) Fully sampled T2-image, (b) undersampling pattern with 25% data sampled, (c) reconstructed image using shift-invariant wavelets with four decomposition levels, (d) reconstructed using PANO with (c) as the guide image, (e) fully sampled T1-image, (d) reconstructed using PANO with (e) as the guide image. The reconstruction error RLNEs of (c), (d) and (f) are 0.18, 0.092, and 0.070.

3.2 Learn similarities from another modal image

For diagnosis, multi-modal MR images may be acquired. Due to the correlated features between these images, it is

possible to incorporate information from one modal image into another modal image.

Assuming that a full T1 weighted image shown in Fig. 1(e) is available, similarities can also be learnt from it then feed it into PANO as prior information. For the given sampling pattern in Fig. 4(b), learning the similarities from this T1 image outperforms learning the similarities from conventional CS-MRI reconstruction since better visual quality and lower reconstruction error are achieved comparing Fig. 4(f) with Fig. 4(d). The same observation is found for realistic MRI data as shown in Fig. 5.

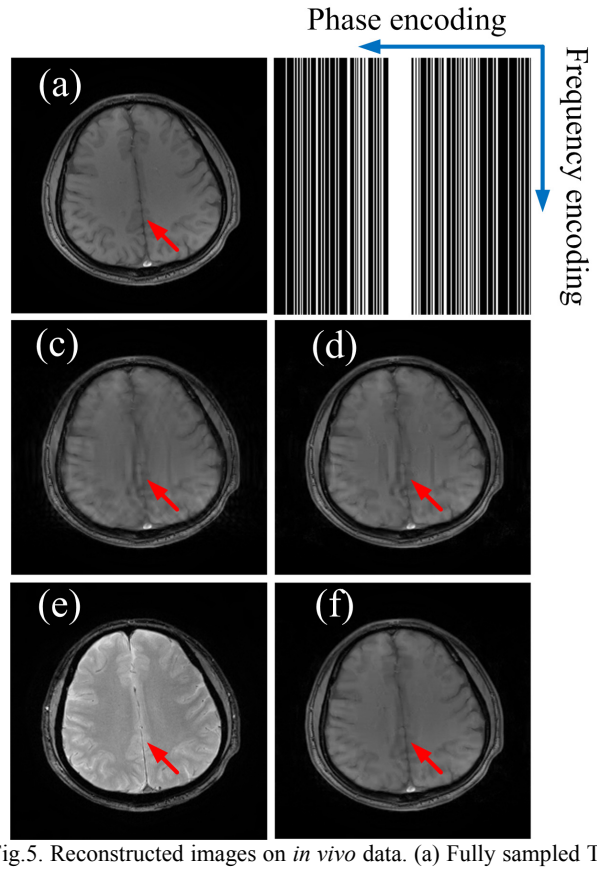

Fig.5. Reconstructed images on *in vivo* data. (a) Fully sampled T2-image, (b) undersampling pattern with 35% data sampled, (c) reconstructed image using shift-invariant wavelets with four decomposition levels, (d) reconstructed using PANO with (c) as the guide image, (e) fully sampled T1-image, (d) reconstructed using PANO with (e) as the guide image. The reconstruction error RLNEs of (c), (d) and (f) are 0.120, 0.081, and 0.062.

4. CONCLUSIONS

A patch-based nonlocal operator (PANO) is established to model the linear representation of image patches. By learning the similarities from guide images, undersampled magnetic resonance image reconstruction using PANO significantly improves the reconstructed images. Learning similarities from another full modal image outperforms learning similarities from undersampled data for the given examples. Further investigation on the proposed method with *in vivo* data is undergoing. More details on PANO-based CS-MRI image reconstruction can be found in [21].

5. ACKNOWLEDGEMENTS

The authors sincerely thank Dr. Feng Huang at Philips Research China for providing the realistic MRI data used in in Fig. 5. This work was supported by the NNSF of China (61201045 and 11174239), Open Fund from Key Lab of Digital Signal and Image Processing of Guangdong Province (54600321), the NSF of Shandong Province (ZR2011FM004), and Scientific Research Foundation for the Introduction of Talent at Xiamen University of Technology (90030606).

6. REFERENCES

[1] M. Lustig, D. Donoho, and J. M. Pauly, "Sparse MRI: The application of compressed sensing for rapid MR imaging," *Magnetic Resonance in Medicine,* vol. 58, pp. 1182-1195, 2007.

[2] X. B. Qu, W. R. Zhang, D. Guo, C. B. Cai, S. H. Cai, and Z. Chen, "Iterative thresholding compressed sensing MRI based on contourlet transform," *Inverse Problems in Science and Engineering,* vol. 18, pp. 737-758, 2010.

[3] F. Knoll, K. Bredies, T. Pock, and R. Stollberger, "Second order total generalized variation (TGV) for MRI," *Magnetic Resonance in Medicine,* vol. 65, pp. 480-491, 2011.

[4] X. B. Qu, X. Cao, D. Guo, C. W. Hu, and Z. Chen, "Combined sparsifying transforms for compressed sensing MRI," *Electronics Letters,* vol. 46, pp. 121-122, 2010.

[5] Y. M. Chen, X. J. Ye, and F. Huang, "A novel method and fast algorithm for MR image reconstruction with significantly under-sampled data," *Inverse Problems and Imaging,* vol. 4, pp. 223-240, 2010.

[6] S. Ravishankar and Y. Bresler, "MR image reconstruction from highly undersampled k-space data by dictionary learning," *IEEE Transactions on Medical Imaging,* vol. 30, pp. 1028-1041, 2011.

[7] E. V. R. DiBella and G. Adluru, "Reordering for improved constrained reconstruction from undersampled k-space data," *International Journal of Biomedical Imaging,* vol. 2008, Article ID 341684, 2008.

[8] B. Wu, R. P. Millane, R. Watts, and P. J. Bones, "Prior estimate-based compressed sensing in parallel MRI," *Magnetic Resonance in Medicine,* vol. 65, pp. 83-95, 2011.

[9] X. B. Qu, D. Guo, B. D. Ning, Y. K. Hou, Y. L. Lin, S.H. Cai, and Z. Chen, "Undersampled MRI reconstruction with

patch-based directional wavelets," *Magnetic Resonance Imaging,* vol. 30, pp. 964-977, 2012.

[10] H. Q. Du and F. Lam, "Compressed sensing MR image reconstruction using a motion-compensated reference," *Magnetic Resonance Imaging,* vol. 30, pp. 954-963, 2012.

[11] G. Adluru, T. Tasdizen, M. C. Schabel, and E. V. R. DiBella, "Reconstruction of 3D dynamic contrast-enhanced magnetic resonance imaging using nonlocal means," *Journal of Magnetic Resonance Imaging,* vol. 32, pp. 1217-1227, 2010.

[12] D. Liang, H.F. Wang, Y. C. Chang, and L. Ying, "Sensitivity encoding reconstruction with nonlocal total variation regularization," *Magnetic Resonance in Medicine,* vol. 65, pp. 1384-1392, 2011.

[13] S. Fang, K. Ying, L. Zhao, and J. P. Cheng, "Coherence regularization for SENSE reconstruction with a nonlocal operator (CORNOL)," *Magnetic Resonance in Medicine,* vol. 64, pp. 1414-1426, 2010.

[14] A. Wong, A. Mishra, P. Fieguth, and D. Clausi, "Sparse reconstruction of breast MRI using homotopic L_0 minimization in a regional sparsified domain," *IEEE Transactions on Biomedical Engineering,* vol. 60, pp.743-752, 2013.

[15] K. Egiazarian, A. Foi, and V. Katkovnik, "Compressed sensing image reconstruction via recursive spatially adaptive filtering," in *14th IEEE International Conference on Image Processing, ICIP 2007, September 16, 2007 - September 19, 2007*, IEEE, San Antonio, TX, United states, pp. 549-552, 2006.

[16] M. Akçakaya, T. A. Basha, B. Goddu, L. A. Goepfert, K. V. Kissinger, V. Tarokh, W. J. Manning, and R. Nezafat, "Low-dimensional-structure self-learning and thresholding: Regularization beyond compressed sensing for MRI Reconstruction," *Magnetic Resonance in Medicine,* vol. 66, pp. 756-767, 2011.

[17] J. F. Yang, Y. Zhang, and W.T. Yin, "A Fast TVL1-L2 minimization algorithm for signal reconstruction from partial Fourier data," *Technical Report*, Rice University, 2009.

[18] K. Dabov, A. Foi, V. Katkovnik, and K. Egiazarian, "Image denoising by sparse 3-D transform-domain collaborative filtering," *IEEE Transactions on Image Processing,* vol. 16, pp. 2080-2095, 2007.

[19] J. V. Manjn, N. A. Thacker, J. J. Lull, G. Garcia-Marti, L. Marti-Bonmati, and M. Robles, "Multicomponent MR image denoising," *International Journal of Biomedical Imaging,* Article ID 756897, 2009.

[20] C. A. Cocosco, V. Kollokian, Kwan, and A. C. Evans, "BrainWeb: Online interface to a 3D MRI simulated brain database," *Neuroimage,* vol. 5, p. S425, 1997.

[21] X. B. Qu, Y. K. Hou, F. Lam, D. Guo, J. H. Zhong, and Z. Chen, "Magnetic resonance image reconstruction from undersampled measurements using a patch-based nonlocal operator", *submitted to Medical Image Analysis*, 2013.